

NEDO-25090  
79NED053  
CLASS I  
MAY 1979

# ANALYTICAL MODELS FOR T-QUENCHER WATER JET LOADS ON SUBMERGED STRUCTURES

TASK 5.14.2

497 083

GENERAL  ELECTRIC

7907160334

NEDO-25090  
Class I  
May 1979

ANALYTICAL MODEL FOR T-QUENCHER WATER JET LOADS ON SUBMERGED STRUCTURES  
TASK 5.14.2

F. T. Dodge  
SwRI Project 02-5352  
G.E. P.O. 205-G7F70

Reviewed by:

L. Lasher  
L. Lasher, Senior Engineer  
Containment Methods

A. E. Rogers  
A. E. Rogers, Manager  
Containment Technology

Approved by:

P. W. Ianni  
P. W. Ianni, Manager  
Containment Design

NUCLEAR ENERGY ENGINEERING DIVISION • GENERAL ELECTRIC COMPANY  
SAN JOSE, CALIFORNIA 95125

GENERAL  ELECTRIC

497 084

## DISCLAIMER OF RESPONSIBILITY

*This document was prepared by or for the General Electric Company. Neither the General Electric Company nor any of the contributors to this document:*

- A. Makes any warranty or representation, express or implied, with respect to the accuracy, completeness, or usefulness of the information contained in this document, or that the use of any information disclosed in this document may not infringe privately owned rights; or*
- B. Assumes any responsibility for liability or damage of any kind which may result from the use of any information disclosed in this document.*

*Proprietary information of the General Electric Company is indicated by "bars" drawn in the margin of the text of this report, and by the words "Company Proprietary" in illustration and table titles.*

## TABLE OF CONTENTS

	Page
1. INTRODUCTION	1-1
1.1 General Approach	1-1
1.2 Quencher Geometry	1-4
2. DYNAMICS OF QUENCHER ARM JET	2-1
2.1 Orifice Jets	2-1
2.2 Column Jets	2-4
2.2.1 Isolated Column Region	2-4
2.2.2 Merged Column Region	2-7
2.3 Quencher Arm Jet	2-8
2.4 Transient Decay of Quencher Jet	2-9
3. JET PENETRATION	3-1
4. SUMMARY OF RESULTS OF QUENCHER ARM JET	4-1
5. NUMERICAL EXAMPLE OF QUENCHER JET	5-1
6. END CAP JET	6-1
6.1 Orifice Jets Merge to Form a Column Jet	6-1
6.2 Column Jets Merge to Form an End Cap Jet	6-2
6.3 End Cap Jet	6-3
6.4 Transient Decay of End Cap Jet	6-5
7. SUMMARY OF RESULTS FOR END CAP JET	7-1
8. NUMERICAL EXAMPLE FOR END CAP JET	8-1
9. FORCE PREDICTIONS	9-1

TABLE OF CONTENTS (Continued)

	Page
10. REFERENCES	10-1
APPENDIX A	
MODIFIED ANALYTICAL MODEL FOR T-QUENCHER WATER JET LOADS ON SUBMERGED STRUCTURES	A-1

497 087

## LIST OF ILLUSTRATIONS

<u>Figure</u>	<u>Title</u>	<u>Page</u>
1	Phases of Quencher Jet Formation and Decay	1-5
2	Typical T-Quencher Arm	1-7
3	Interaction of Orifice Jets	2-11
4	Column Jets	2-12
5	"Wake" Behavior of Merging Column Jets	2-13
6	Quencher Arm Jet	2-14
7	Quencher Jet Velocity vs Downstream Distance	5-3
8	Possible Structure/Jet Interactions	9-2

## LIST OF SYMBOLS

$B$	width of quencher arm jet
$l$	"mixing length" for wake analyses
$\dot{M}$	entrained mass flow rate
$\dot{m}_{en}$	entrained mass flow rate per orifice
$r$	radial coordinate from jet centerline
$r_o$	orifice radius
$r_{1/2}, r_{1/10}$	width of orifice jet at which velocity is one-half or one-tenth, respectively, of the centerline velocity
$t$	time
$t_o$	time at which water flow through orifices ceases
$V$	jet velocity at arbitrary point
$V_c$	jet centerline velocity
$V_i$	initial velocity of column jet
$V_{QA_o}$	initial velocity of quencher arm jet
$V_{QA}$	quencher arm jet velocity
$V_{Q_o}$	quencher arm jet velocity at $t = t_c$
$W$	height of quencher arm jet
$x$	distance downstream from quencher arm periphery
$\bar{x}$	distance downstream from column jet origin
$X_m$	downstream distance at which orifice jets merge
$X_T$	downstream distance at which column jets merge
$X_o$	quencher jet penetration at $t = t_o$
$X_{TOTAL}$	total penetration of quencher jet

$\bar{y}_{1/2}$	width of column jet at which velocity is one-half of the centerline velocity
$\bar{z}$	downstream distance for "wake" analysis
$\rho$	liquid density
$\lambda$	spacing between column jets

## 1. INTRODUCTION

### 1.1 GENERAL APPROACH

An analytical method is presented herein to compute bounding loads on underwater structures due to water jets from a T-quencher type S/RV discharge device. The general approach uses analytical and experimental results for steady-state jets that are available in the open literature.

The quencher jet is comprised of a series of constituent jets characteristic of the region in which they develop. Each of the component jets is analyzed resulting in predictions of jet velocities and zones of influence. The penetration distance of the jet is determined from a scaled flow-visualization experiment. A similar analysis is performed for the end-cap design of the quencher containing orifices.

A simple steady-state drag equation is used to predict the submerged-structure loads from the calculated velocities.

Appendix A provides a modified analytical model that accounts for the non-uniform hole spacing and is a recommended procedure for Mark I T-quencher water-jet load predictions.

Actuation of a safety/relief valve discharges the water contained in the piping through the many orifices in the quencher arms. The circular jets formed by the flow from each arm entrain water in the pool to form a much larger, radially-expanding rectangular jet which has the same total momentum as the sum of the momenta of the individual circular jets. Figure 1 describes in a general way these various phenomena. Significant loads on structures submerged in the pool may be produced by the water jets, and for that reason an analytical model is needed to estimate the dynamics of the jet. Such a method is developed herein.

The method of approach taken in developing the analytical model for the various phases of jet formation and decay shown in Figure 1 is summarized as follows:

- a) The rate of velocity decay of individual circular "orifice jets" that are formed at each hole and the jet liquid entrainment with distance traveled are determined up to the location where the jets begin to merge.

Since quencher hole spacing in the circumferential direction is smaller than in the axial direction, the orifice jets first merge in the circumferential direction forming rectangular "column jets" at each axial location.

- b) After the orifice jets have merged, the velocity decay and the liquid entrainment of the rectangular column jets formed by the merged orifice jets are determined up to the location where the column jets begin to merge in the axial direction.
- c) After the column jets have merged, the velocity decay and the liquid entrainment of each rectangular "quencher arm jet" are determined up to the time when all the liquid has been exhausted through the holes.
- d) After the flow of liquid through the quencher holes has stopped, the velocity and the penetration distance of the quencher jet are determined with the aid of scale-model test data.

Steady-state submerged-jet theory is used for parts (a) through (c), for two reasons: (1) there is little in the way of theoretical results or experimental correlations for unsteady jets, and (2) a steady-state model will predict larger than actual velocities (i.e., the model will be conservative) because the energy that in fact would be expended in the unsteady formation of the jet is conservatively included in the calculation of the velocity head of the steady jet. Energy expended in the unsteady formation includes that required to establish the flow field as well as that dissipated by the starting vortices during the formation of the orifice jets. All predictions

are based upon the maximum representative orifice velocity rather than some average, which thus gives an additional source of conservatism.

For part (d), steady-state results for velocity decay would be overly conservative. For that reason, scale-model test data are used to develop relations for the jet penetration distance and the rapidly-decaying velocity after the orifice liquid flow has stopped. These tests indicated that the flow field in the pool after the orifice flow stops is primarily the result of the momentum obtained during the preceding quasi-steady flow period. Additional liquid is still entrained by the jet, nonetheless, and this causes the jet velocity to decay rapidly. The flow of air and steam through the quencher holes following the water flow eventually forms large bubbles which then begin to develop a new flow field in the pool. The velocity induced by the water jet is very small by the time the flow induced by the bubbles becomes significant.

## 1.2 QUENCHER GEOMETRY

The quencher jet model is based on a typical T-quencher geometry (see Figure 2). A large number of holes are arranged in columns perpendicular to the quencher arm axis. The distance from the column of holes nearest the ramshead to the column of holes farthest from the ramshead is   \*   in.; total number of columns is   \*  ; spacing between columns is   \*   in., except for a spacing of   \*   in. between columns 18 and 19 and a spacing of   \*   in. between columns   \*   and   \*  ; number of holes per column varies from   \*   for the   \*   columns nearest the ramshead to   \*   for the   \*   columns farthest from the ramshead; angular distance between holes in a column is   \*   for all columns; and hole diameter is   \*   inch. For simplicity, a uniform hole pattern is used here in deriving certain geometric relations in the analytical model:   \*   columns equally spaced at   \*   in., with each column containing   \*   holes. This is an "average" representation of the   \*   columns farthest from the ramshead but overestimates the number of holes in the   \*   columns nearest the ramshead. Quarter-scale model tests showed that air and steam flow almost immediately out of these   \*   columns; since the analytical model assumes that water flows out all orifices for the total time duration, the assumed uniform hole pattern is conservative. The orifice water velocity and total water flow time are based

on the orifices near the center of the arm because, based on the test results, these seem to best represent the characteristics of the discharged water. There are also orifices in the cap at the end of the arm in some designs. The jet formed by the flow out these orifices is treated in Section 6.

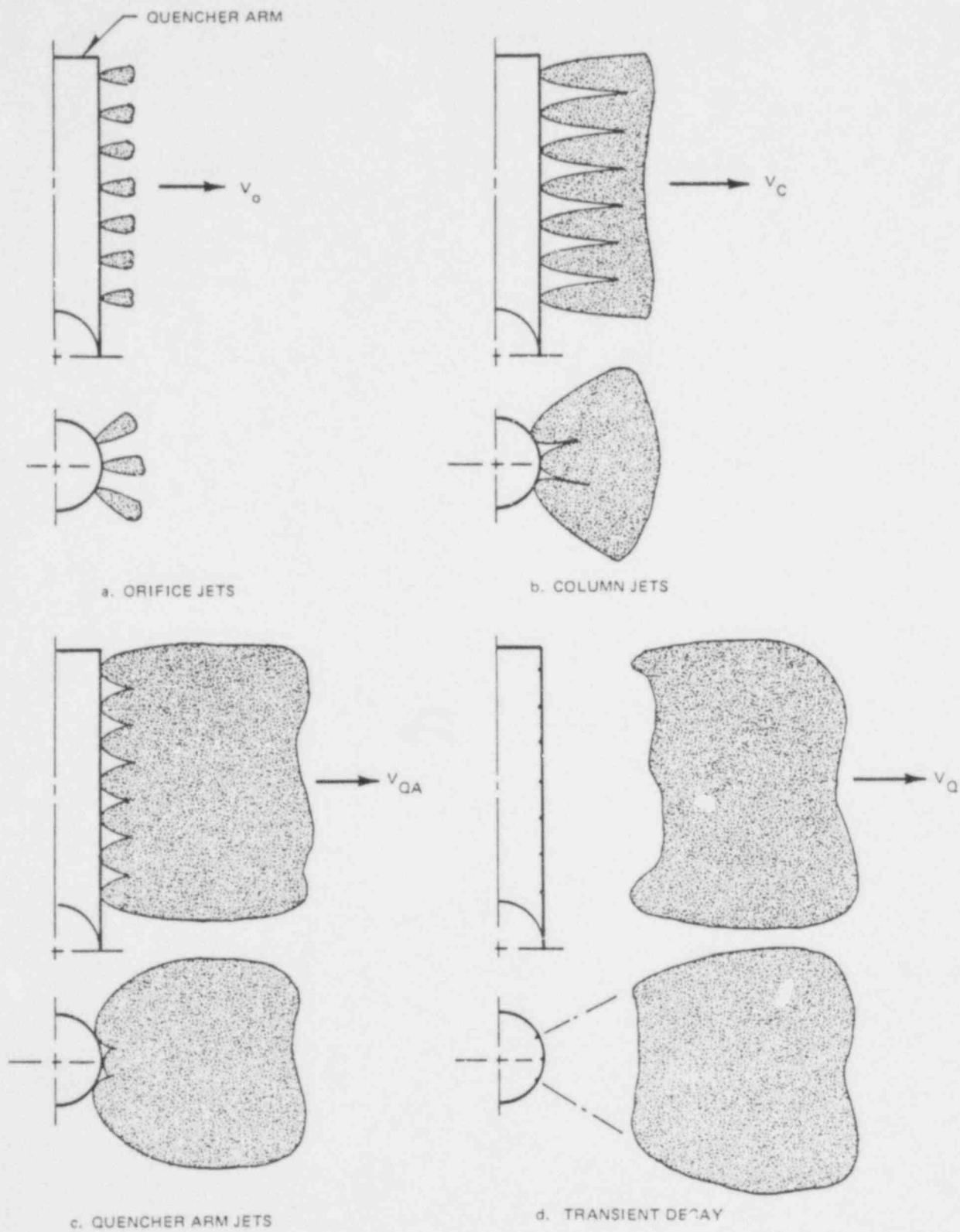


Figure 1. Phases of Quencher Jet Formation and Decay

General Electric  
Company Proprietary

Figure 2. Typical T-Quencher Arm  
(GE Company Proprietary)

2. DYNAMICS OF QUENCHER ARM JET

## 2.1 ORIFICE JETS

Until the water jets formed at each orifice begin to merge, each jet can be considered as steady, axisymmetric, and submerged in an infinitely extending pool of stationary water. Available theories and experimental correlations (references 1, 2, and 3, for example) show that the centerline velocity  $V_c$  of such a jet decreases with the distance traveled from its origin. Of the several forms given for this decrease, an expression derived from a combination of results from references 1 and 2 well represents the experimental data:

$$V_c(x) = 13.14 V_o / (4.39 + x/r_o) \text{ for } x/r_o \geq 8.75 \quad (2.1a)$$

$$V_c(x) = V_o \text{ for } 0 < x/r_o \leq 8.75 \quad (2.1b)$$

$V_o$  is the uniform velocity of the jet at the exit of the orifice, and can be obtained from the model of Reference 4,  $r_o$  is the radius of the orifice, and  $x$  is the downstream distance measured along the jet centerline. The region  $x/r_o < 8.75$  is the "potential core" which is the distance required for viscous shear to penetrate from the jet boundary to the centerline. In this region the centerline (maximum) velocity does not change although the average velocity does (Reference 5).

Equations 2.1 are derived in the following way. Reference 1 gives  $V_c = 13.14 V_o r_o / \bar{x}$  where  $\bar{x}$  is the downstream distance measured from the "virtual origin" of the jet. Reference 2 gives  $V_c = V_o \{1 - \exp[-(0.08 x/r_o - 0.7)^{-1}]\}$  for jet Mach numbers near zero and for equal jet and surrounding fluid densities; the length of the potential core predicted by this expression is  $0.7 r_o / 0.33 = 8.75 r_o$ . These two correlations are combined to give equation 2.1. (The exponential decay rate given in Reference 2 is derived in Reference 3, using slightly different analytical assumptions than those made in Reference 1.

Except in the vicinity of  $x = 8.75 r_o$ , both the exponential decay and equation 2.1 give equivalent numerical predictions for the velocity decrease. Equation 2.1 is a little easier to use in the model developed here.)

The velocity distribution across the jet cross-section is (Reference 1):

$$V(r,x) = V_c(x) \left[ 1 + 57.49 \left/ \left( \frac{r/r_o}{4.39 + x/r_o} \right)^2 \right. \right]^2 \quad (2.2)$$

$$\text{for } x/r_o > 8.75$$

Equation 2.2 is used to compute the radial dimensions of the circular jet. Since it predicts that the jet extends infinitely in the radial direction--although with a negligibly small velocity when  $r/r_o$  is large--it is customary to specify a jet "half width"  $r_{1/2}$  as a measure of the jet size. The half width is defined to be the width at which the velocity is one-half the centerline velocity. From equation 2.2, the half width for a circular jet is:

$$r_{1/2} = 0.0848 r_o (x/r_o + 4.39) \text{ for } x/r_o > 8.75 \quad (2.3)$$

Some other theories assume a Gaussian velocity profile:  $V(r,x) = V_c * \exp[-(r/r_{1/2})^2 \ln 2]$ . In either case, the chosen profile, in conjunction with the form of the centerline velocity decrease, must be such as to conserve the initial momentum  $\rho \pi r_o^2 V_o^2$  of the jet. A Gaussian profile is only slightly different than equation 2.2, and when  $r_{1/2}$  is chosen in accordance with equation 2.3, both profiles conserve jet momentum to within the accuracy of the constant 0.0848.

Equation 2.3 is not valid for  $x/r_o < 8.75$ . The jet still expands in this region, but at a slower rate (Reference 5). For the model developed here, a linear rate of increase with  $x$  is assumed, with the exact form determined by

497 098

requiring that:  $r_{1/2}$  equals equation 2.3 for  $x = 8.75 r_o$ , and  $r_{1/2}$  equals  $r_o$  for  $x = 0$ . Thus,

$$r_{1/2} = r_o (1 + 0.013 x/r_o) \text{ for } 0 \leq x/r_o \leq 8.75 \quad (2.4)$$

Somewhere downstream, the individual orifice jets in a single column will have expanded to such an extent that they begin to interact. From this point on, it is unrealistic to assume that each orifice jet is isolated from the rest. A reasonable way to estimate when this interaction begins to be important is to assume that the jets are no longer isolated when the radii of adjacent jets for which  $V(r,x) = V_c/10$  overlap. (It will be seen that the results are not particularly sensitive to this assumption.) For  $x/r_o > 8.75$ , equation 2.2 shows that  $V = V_c/10$  when  $r = r_{1/10} = 2.29 r_{1/2}$ . For  $x/r_o < 8.75$ , a linear increase of  $r_{1/10}$  is assumed; the conditions used to derive the assumed expression are: (1)  $r_{1/10} = 2.29 r_{1/2}$  for  $x = 8.75 r_o$ , and (2)  $r_{1/10} = r_o$  for  $x = 0$  (the velocity decreases from the maximum to zero over a very short radial distance at the orifice exit). The derived expression is  $r_{1/10} = r_o (1 + 0.177 x/r_o)$  for  $x/r_o < 8.75$ . With reference to Figure 3, the distance  $X_m$  at which the orifice jets merge can thus be found either from:

$$r_o [1 + 0.177(X_m/r_o)] = (L_1/2 + X_m \sin 2.7^\circ) / \cos 2.7^\circ \quad (2.5a)$$

if  $X_m < 8.75 r_o$ , or from

$$2.29 r_o [0.0848(X_m/r_o + 4.39)] = (L_1/2 + X_m \sin 2.7^\circ) / \cos 2.7^\circ \quad (2.5b)$$

if  $X_m \geq 8.75 r_o$ . Since  $r_o = 0.1955$  in. and  $L_1 = 0.60$  in., the solution to these equations is  $X_m = 0.807$  in.  $= 4.1 r_o$ , which agrees reasonably well with the SWRI scale-model tests. (If  $V = 0.01 V_c$  is chosen to compute the interaction location, the solution is  $X_m = 3.3 r_o$ . Thus, the result is not sensitive to this assumption.)

The liquid entrained by the circular jet up to  $x = 4.1 r_o$  is small compared to the initial liquid flow, and so is not presented here.

## 2.2 COLUMN JETS

The column jet formed by the orifice jets merged in the circumferential direction is analyzed here as an expanding, submerged, rectangular jet; see Figure 4.

### 2.2.1 Isolated Column Region

The first part of the analysis determines the downstream location where the column jets begin to merge in the axial direction. For this purpose only, it is assumed that the diffusion of momentum in the axial direction and the liquid entrainment between the jets is independent of the geometric divergence of the column height,  $W$ , with downstream distance. Hence, available theories for a rectangular jet of constant height can be used; these show that the decrease of centerline velocity is (Reference 6):

$$V_c(\bar{x}) = 2.53 V_i / (\bar{x}/d_o + 0.6)^{1/2} \quad \text{for } \bar{x}/d_o \geq 5.8 \quad (2.6)$$

and the jet half width  $\bar{y}_{1/2}$  is

$$\bar{y}_{1/2} = 0.1038 d_o (\bar{x}/d_o + 0.6) \quad \text{for } \bar{x}/d_o > 5.8 \quad (2.7)$$

The velocity profile is

$$V(\bar{y}, \bar{x}) = V_c(\bar{x}) \exp \left[ -(\bar{y}/\bar{y}_{1/2})^2 \ln 2 \right] \quad \text{for } \bar{x}/d_o \geq 5.8 \quad (2.8)$$

Here,  $\bar{x}$  is the downstream distance from the rectangular jet origin, where  $\bar{x} = 0$  corresponds to  $x = 4.10 r_o$  of the coordinate system whose origin is at the orifice exit, and  $d_o = 2.107 r_o$  is the initial width of the column jet, which is assumed to be twice the half width of the orifice jets at  $x = 4.10 r_o$ . The downstream distance at which a column jet can no longer be

assumed to be isolated is again taken as the point where the velocity  $V = V_c/10$  of adjacent jets overlap.  $V = V_c/10$  occurs for  $\tilde{y} = 1.82 \tilde{y}_{1/2}$ , from equation 2.8, so the distance  $X_T$ , measured from the orifice exits where the column jets begin to interact is:

$$1.82 \left[ 0.1038 \left( \frac{X_T - 4.10 r_o}{2.107 r_o} + 0.6 \right) (2.107 r_o) \right] = L_2/2 \quad (2.9)$$

For  $L_2 = \underline{\quad}$  in.,  $X_T = 5.77$  in.  $= 29.5 r_o$ . From this point on, the column jets are no longer isolated.

The geometric divergence of the column jet height in the region  $4.10 r_o \leq x \leq 29.5 r_o$  must be taken into account in determining the true jet velocity; equation 2.6, recall, neglects the geometric divergence. There are no exact results available for a diverging rectangular jet, but the divergence effect can be computed approximately by balancing the jet momentum, temporarily neglecting the transverse turbulent diffusion. The momentum balance is  $\rho A_1 V_1^2 = \rho A V^2$  or  $V = V_1 \sqrt{A_1/A}$ . The increase in jet height (i.e., area) is proportional to  $x$ , so the velocity must decrease in proportion to  $1/\sqrt{x}$ . Using this fact, and now including the transverse diffusion (but neglecting any additional lateral diffusion) gives:

$$V_{CJ} = V_i \left[ \frac{10 L_1 + 2 r_o + 4.10 r_o \left( \frac{54\pi}{180} \right)}{10 L_1 + 2 r_o + x (54\pi/180)} \right]^{1/2} \quad (2.10)$$

$$= V_i \left[ \frac{38.803}{34.703 + x/r_o} \right]^{1/2}$$

for  $4.10 r_o \leq x \leq 5.8 d_o + 4.10 r_o = 16.23 r_o$ , and

$$V_{CJ} = 2.53 V_i \left[ \frac{38.803}{34.703 + x/r_o} \right]^{1/2} \left( \frac{x/r_o - 4.10}{2.107} + 0.6 \right)^{1/2} \quad (2.11)$$

for  $16.28 r_o \leq x \leq 29.5 r_o$ . In equation 2.11, the last term represents the centerline velocity decay due only to transverse diffusion.

The initial velocity  $V_i$  is obtained from a balance of momentum with the orifice jets. This is slightly in error because it produces an artificial drop in jet velocity at  $x = 4.10 r_o$ , which is the matching point between the orifice and the column jet models; however, it gives the correct results not too far downstream of  $x = 4.10 r_o$ . Thus:

$$(11) \quad (\pi r_o^2 V_o^2) = \rho V_i^2 \left[ 10 L_1 + 2 r_o + 4.10 r_o \left( \frac{54\pi}{180} \right) \right] (2.107 r_o)$$

or

$$V_i = 0.670 V_o \quad (2.12)$$

Using the above equations, the liquid entrained by the jets can be estimated. For example, in the region  $x > 16.28 r_o$  (the fully developed column jet), the total liquid flow entrained per column is:

$$\dot{m}_{en} = \rho V_{CJ} \left[ (2.107 r_o) (10 L_1 + 2 r_o + 0.942 x) \right] - 11 (\rho V_o r_o^2) \quad (2.13)$$

where  $V_{CJ}$  is computed from equation 2.11. Expressing the entrainment on a per orifice basis gives:

$$\dot{m}_{en} = \left[ 0.0610 \frac{V_{CJ}}{V_o} \left( 10 \frac{L_1}{r_o} + 2 + 0.942 \frac{x}{r_o} \right) - 1 \right] \pi r_o^2 V_o \quad (2.14)$$

At the point where the columns merge,  $x = 29.5 r_o$ , the entrained flow is  $0.367 \pi r_o^2 V_o$  per orifice, about one-third of the initial flow.

497 102

2.2.2 Merged Column Region

After the column jets interact downstream of  $x = 29.5 r_o$ , all the water between the columns is accelerated by exchanging momentum with the jets, and the column jets cannot be considered as isolated. A reasonable model of the interchange is to treat it as a periodic wake in which the entire velocity profile in the spaces between the jets begins to smooth out toward an eventual uniform profile (see Figure 5).

According to Reference 1, the rate at which the wake velocity approaches uniformity can be estimated from

$$\frac{\Delta V}{V_{QA_o}} = \frac{1}{8\pi^3} \left( \frac{L_2}{\ell} \right)^2 \left( \frac{L_2}{\bar{z}} \right) \cos(2\pi \bar{y}/L_2) \text{ for } \bar{z}/L_2 > 4 \quad (2.15)$$

Here  $\Delta V$  is the difference between the wake velocity and the eventual uniform velocity  $V_{QA_o}$ ,  $L_2 = \underline{\quad}$  in. is the spacing between orifice columns,  $\bar{z}$  is the downstream distance, and  $\ell = 0.103 L_2$  is the relevant "mixing length" for this model. The profile is essentially uniform when  $\Delta V < 0.1 V_{QA_o}$ , or when:

$$\bar{z}_{\text{merge}} = 7.49 \text{ in.} = 38.3 r_o \quad (2.16)$$

Thus, the column jets have totally merged to form a single "quencher arm jet" at a distance of  $29.5 r_o + 38.3 r_o = 67.8 r_o$  downstream of the orifices.

The uniform velocity at the end of the wake region is determined from a balance of momentum with all the orifice jets comprising it:

$$(47 \times 11) \rho \pi r_o^2 V_o^2 = (46 L_2 + 2 r_o) * \left[ 10 L_1 + 2 r_o + 67.8 r_o \left( \frac{54\pi}{180} \right) \right] * \rho V_{QA_o}^2$$

or

$$V_{QA_0} = 0.191 V_0 \quad (2.17)$$

$V_{QA_0}$  is also the initial velocity of the quencher jet. The liquid flow entrained up to this point is  $4.24 \pi r_0^2 V_0$  per orifice.

The velocity decrease in the wake region can be estimated from the form of equation 2.15)--that is, the velocity decreases in proportion to  $1/x$ . Since the velocity is  $0.37 V_0$  at the start of the wake (equation 2.11) and  $0.191 V_0$  at the end (equation 2.17), the velocity decrease prediction is:

$$V_{\text{wake}} = 14.96 V_0 / (x/r_0 + 10.93) \text{ for } 29.5 \leq x/r_0 \leq 67.8 \quad (2.18)$$

### 2.3 QUENCHER ARM JET

The upper and lower boundaries of the fully-merged column jet continue to diverge at least at the  $54^\circ$  angle included between the upper and lower rows of orifices in the quencher arm; in fact, the 1/4 scale-model tests indicate that the divergence may even be greater than  $54^\circ$ . For the model developed here, the divergence is assumed to be  $54^\circ$ , which, therefore, gives a conservative result for the velocity. The velocity decrease with distance of the quencher arm jet can be computed from a momentum balance. With reference to Figure 6, the momentum balance is:

$$(47 \times 11) \pi r_0^2 V_0^2 = \rho V_{QA}^2 (46 L_2 + 2 r_0) * \left[ 10 L_1 + 2 r_0 + \right. \\ \left. \times \left( \frac{54\pi}{180} \right) \right] \quad (2.19)$$

The quencher arm velocity can therefore be expressed as:

$$V_{QA} = 1.938 V_0 / [34.70 + x/r_0]^{1/2} \text{ for } x/r_0 > 67.8 \quad (2.20)$$

The liquid entrainment per orifice is:

$$\dot{m}_{en} = [0.521 \sqrt{34.66 + x/r_o} - 1] \rho \pi r_o^2 V_o \quad (2.21)$$

#### 2.4 TRANSIENT DECAY OF QUENCHER JET

SwRI scale-model tests showed that the quencher arm jet is engulfed in the air-bubble flow field at a time when the jet velocity has dissipated practically to zero, as was discussed more fully in an earlier section. From the scale-model test data, a conservative estimate of the time required for the quencher jet to decay to a negligible velocity is that the decay time is equal to the preceding liquid flow time through the orifices. In other words, if water flows through the orifices for a time  $t_o$  and then stops, the quencher jet flow field persists for an additional time  $t_o$ .

It is further assumed that the jet velocity for  $t_o \leq t \leq 2t_o$  decreases with time at a linear rate and is equal to zero for  $t = 2t_o$ . (A linear decrease of velocity with distance gives a smaller jet velocity and, thus, is less conservative.). The approximate expression for the quencher arm jet velocity during the transient decay, then, is:

$$V_Q = V_{Q_o} \left( \frac{2t_o - t}{t_o} \right) \text{ for } t \geq t_o \quad (2.22)$$

where  $V_{Q_o}$  is the value of  $V_Q$  at time  $t = t_o$ . (It is assumed that the water jet leading edge is in the quencher arm jet region when the orifice flow stops; numerical examples for typical conditions show this to be the case.)

Since  $dx = V_Q dt$ , equation 2.22 can be used to derive the velocity-distance relation during the transient decay:

$$V_Q = V_{Q_o} \left[ \frac{V_{Q_o} t_o - 2(x - X_o)}{V_{Q_o} t_o} \right]^{1/2} \text{ for } x > X_o \quad (2.23)$$

Here,  $X_0$  is the location of the leading edge of the quencher arm jet at time  $t = t_0$ .  $V_{Q_0}$  can be computed by substituting  $x = x_0$  into equation 2.20.

497. 106

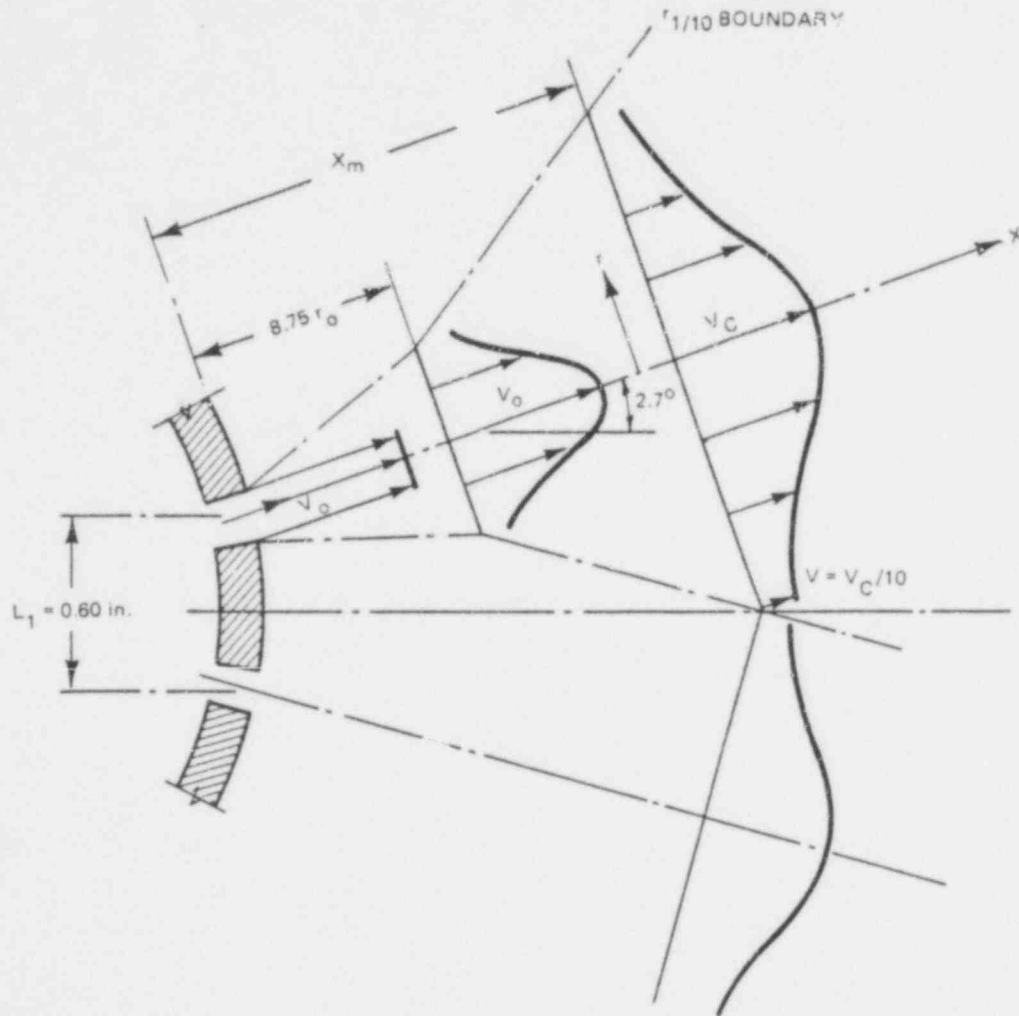


Figure 3. Interaction of Orifice Jets

NOTE: THERE ARE ELEVEN ORIFICE JETS PER COLUMN JET. FOR CLARITY, ONLY FOUR ARE SHOWN

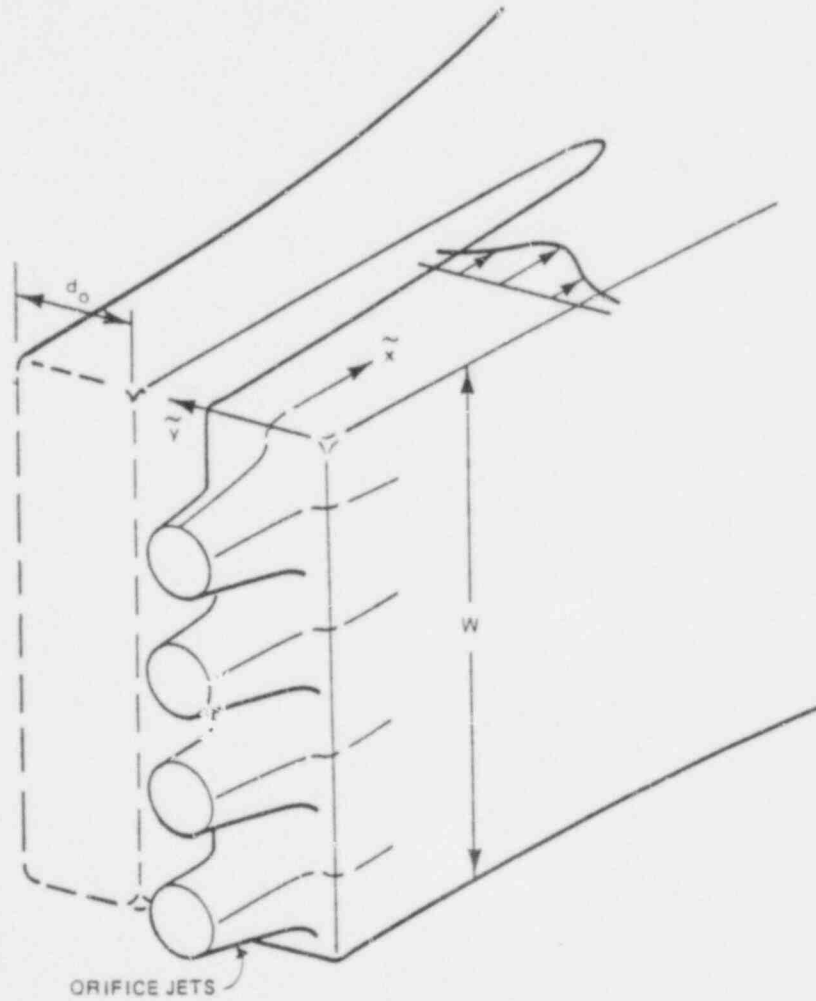


Figure 4. Column Jets

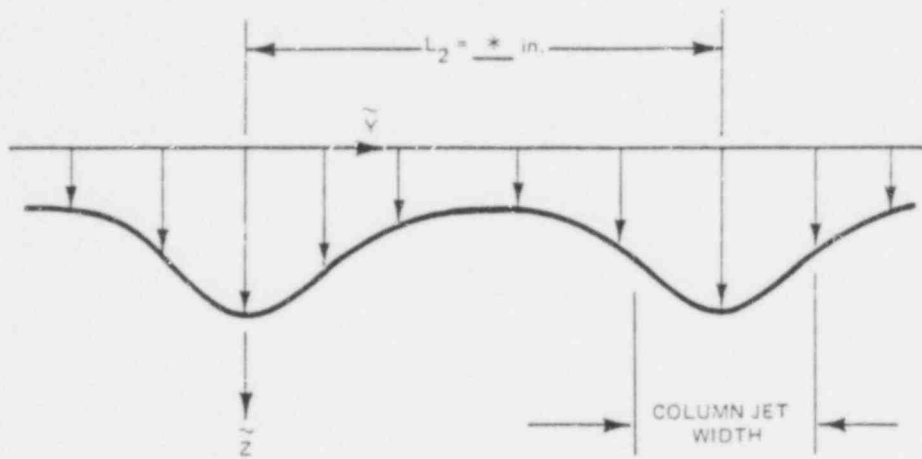


Figure 5. "Wake" Behavior of Merging Column Jets

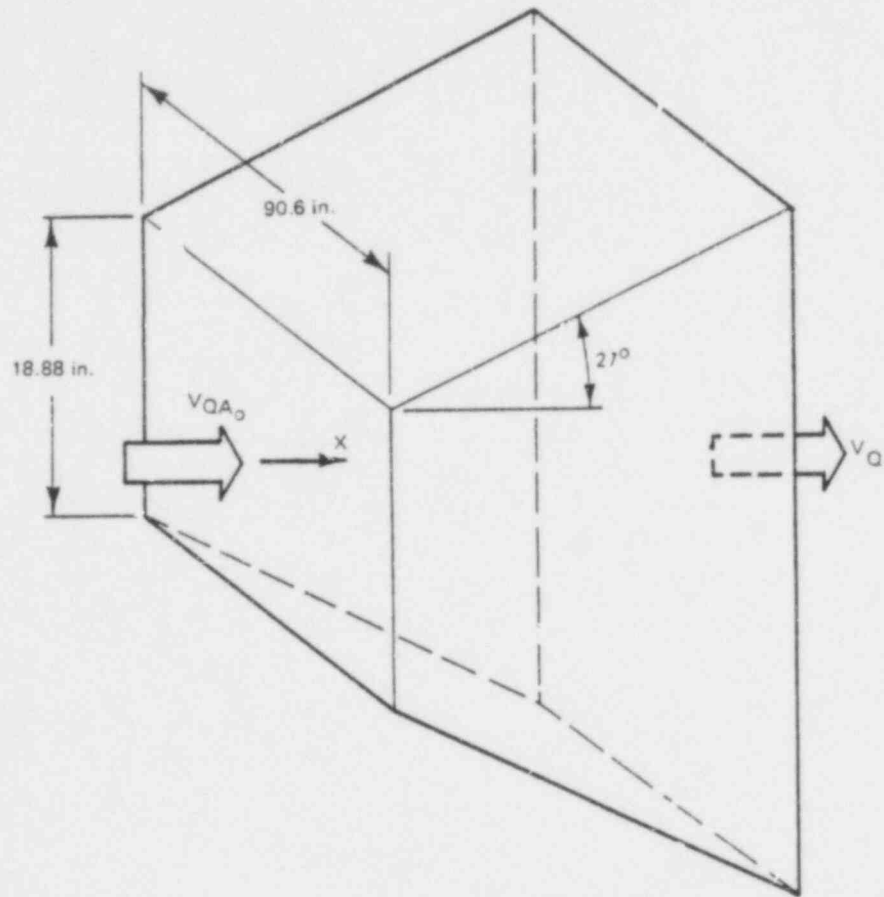


Figure 6. Quencher Arm Jet

3. JET PENETRATION

The total extent of the jet influence - that is, the jet penetration distance - is an important parameter which must be determined. This can be accomplished with the aid of the preceding jet-velocity models.

From equation 2.23, the jet velocity is zero when the leading edge is at  $x = X_o + 1/2 (V_{Q_o} t_o)$ ; this, then, is the total penetration distance, measured from the orifices. That is:

$$X_{TOTAL} = X_o + \frac{1}{2} V_{Q_o} t_o \tag{3.1}$$

The penetration parameter  $X_o$  is computed by determining the time required for the leading edge of the jet to reach the location  $x = X_o$ , which is the sum of the times required for the leading edge to travel through the separate regions of the jet development, each of which is simply  $t = \int dx/V$ , where the integration is performed along the relevant jet centerline. Thus, the total time required for the jet to reach  $x = X_o$  is:

$$\begin{aligned}
 t_o = & \frac{4.1 r_o}{V_o} + \int_{4.1 r_o}^{16.3 r_o} \frac{dx}{0.67 V_o [38.803/(34.703 + x/r_o)]^{1/2}} \\
 & + \int_{16.3 r_o}^{29.5 r_o} \frac{\left[ \frac{x/r_o - 4.1}{2.107} + 0.6 \right]^{1/2} dx}{2.53(0.67 V_o) [38.803/(34.703+x/r_o)]^{1/2}} \\
 & + \int_{29.5 r_o}^{67.8 r_o} \frac{(x/r_o + 10.93) dx}{14.96 V_o} + \int_{67.8 r_o}^{X_o} \frac{[34.66 + x/r_o]^{1/2} dx}{1.938 V_o} \tag{3.2}
 \end{aligned}$$

After integrating:

$$\frac{t_o V_o}{r_o} = 4.1 + 19.57 + 29.43 + 152.53 - 356.77$$

$$+ 0.343997 \left( \frac{x_o}{r_o} + 34.70 \right)^{3/2} \quad (3.3)$$

Solving for  $x_o$ :

$$x_o = \left[ 2.037 \left( \frac{t_o V_o}{r_o} + 151.13 \right)^{2/3} - 34.70 \right] r_o \quad (3.4)$$

Equation 3.4 is valid for orifice flow times  $t_o \geq 205.6 r_o/V_o$ .

When  $x = x_o$  is substituted into equation 2.20, the result is:

$$V_{Q_o} = 1.358 V_o / \left( \frac{t_o V_o}{r_o} + 151.13 \right)^{1/3} \quad (3.5)$$

Therefore, the total penetration distance can be written as:

$$x_{TOTAL} = \left\{ \left[ 2.037 \left( \frac{t_o V_o}{r_o} + 151.13 \right)^{2/3} - 34.70 \right] \right.$$

$$\left. + 0.679 \frac{V_o t_o}{r_o} / \left( \frac{t_o V_o}{r_o} + 151.13 \right)^{1/3} \right\} r_o \quad (3.6)$$

There are no available theories or quantitative test data to describe the mass entrainment or spreading of the jet in this region. It is suggested that the spreading (i.e., the divergence of the jet boundaries) be estimated by the quencher arm jet results.

4. SUMMARY OF RESULTS FOR QUENCHER ARM JET

A summary of the previous models of jet velocity and jet size is presented below.

- $0 \leq x \leq 4.1 r_o$  (orifice jets)  
 $V = V_o$   
 $r_{1/2} = [1 + 0.013 (x/r_o)] r_o$
- $4.1 r_o \leq x \leq 29.5 r_o$  (column jets)  
 $V = 0.67 V_o [38.80 / (34.70 + x/r_o)]^{1/2}$   
 $W = 0.942 r_o (34.70 + x/r_o)$   
 $2 y_{1/2} = 2.107 r_o [1 + 0.027 (x/r_o - 4.1)]$

for  $4.1 \leq x/r_o \leq 16.3$ , and

$$V = 1.695 V_o [38.803 / (34.70 + x/r_o)]^{1/2} / \left[ \frac{x/r_o - 4.1}{2.107} + 0.6 \right]^{1/2}$$

$$W = 0.942 r_o (34.70 + x/r_o)$$

$$2 y_{1/2} = 0.437 r_o \left[ \frac{x/r_o - 4.1}{2.107} + 0.6 \right]$$

for  $16.3 \leq x/r_o \leq 29.5$ .

The first expression for the column jet width has been derived by fitting a linear rate of expansion between the initial width  $d_o$  and the expression for  $2 y_{1/2}$  from equation 2.7.

- $29.5 r_o \leq x \leq 67.8 r_o$  (column jets merging)

$$V = 14.96 / (x/r_o + 10.93)$$

$$W = 0.942 r_o (34.70 + x/r_o)$$

$$B = 463.4 r_o$$

The slight increase of the width and height of the jet due to turbulent diffusion has been neglected.

- $67.8 r_o \leq x \leq \left[ 2.037 \left( \frac{t_o V_o}{r_o} + 151.1 \right)^{2/3} - 34.7 \right] r_o$   
(quencher jet)

$$V = 1.938 V_o / (34.70 + x/r_o)^{1/2}$$

$$W = 0.942 r_o (34.7 + x/r_o)$$

$$d_H = 463.4 r_o$$

When  $x$  is equal to the upper limit, the orifice water flow has just ceased.

- $\left[ 2.037 \left( \frac{t_o V_o}{r_o} + 151.1 \right)^{2/3} - 34.7 \right] r_o \leq x \leq X_{TOTAL}$

$$V = V_{Q_o} \left[ \frac{V_{Q_o} t_o - w(x - X_o)}{V_{Q_o} t_o} \right]$$

$$W = 0.942 r_o (34.70 + x/r_o)$$

$$B = 463.4 r_o$$

where

$$v_{Q_o} = 1.358 v_o / \left( \frac{t_o v_o}{r_o} + 151.1 \right)^{1/3}$$

$$x_o = \left[ 2.037 \left( \frac{t_o v_o}{r_o} + 151.1 \right)^{2/3} - 34.7 \right] r_o$$

$$x_{TOTAL} = \left\{ \frac{2.716 \left( \frac{t_o v_o}{r_o} + 113.35 \right)}{\left( \frac{t_o v_o}{r_o} + 151.1 \right)^{1/3}} - 34.7 \right\} r_o$$

These expressions describe the jet behavior after the water flow through the orifices has ceased.

5. NUMERICAL EXAMPLE OF QUENCHER JET

Typical parameters are:

$$V_o = 200 \text{ ft/sec}$$

$$t_o = 0.18 \text{ sec}$$

$$r_o = \underline{\quad * \quad} \text{ in.}$$

Using these data, at  $t = 0.18 \text{ sec}$  the jet has penetrated a distance:

$$X_o = 326.5 r_o = 5.72 \text{ ft}$$

and has a velocity

$$V_{Q_o} = 0.102 V_o = 20.4 \text{ ft/sec}$$

The total penetration of the jet is:

$$X_{\text{TOTAL}} = 439.1 r_o = \underline{\quad * \quad} \text{ ft}$$

or slightly less than one orifice arm length. This agrees approximately with 1/4 scale model data, although it is conservative (i.e., too large) by about 25%. Note that the bulk of the penetration occurs in the "fully developed" quencher jet region,  $x > 67.8 r_o$ .

The overall jet velocity as a function of downstream distance is shown in Figure 7. The discontinuities shown in the slope of the velocity curve are a result of patching together different theories for different sorts of jets; in practice, these discontinuities would be smoothed, but the magnitude of the velocity would not be significantly different. In particular, the discontinuous drop in velocity from the initial 200 ft/sec to about 135 ft/sec is a result of patching together the axisymmetric orifice jet model to the column jet model. Although such a discontinuous change in velocity is clearly unrealistic, the patching together of the two separate jet models was done by satisfying conservation of momentum, so it is expected that the

predictions become realistic shortly downstream of the patching point,  $x = 4.1 r_0$ . The predicted velocity at  $x \geq 67.8 r_0$  (which is the end of the column jet mixing region) is comparable to the predicted velocity for an axisymmetric jet which is shown in Figure 7 as the dashed line. This lends credibility to the conclusion that the results are realistic.

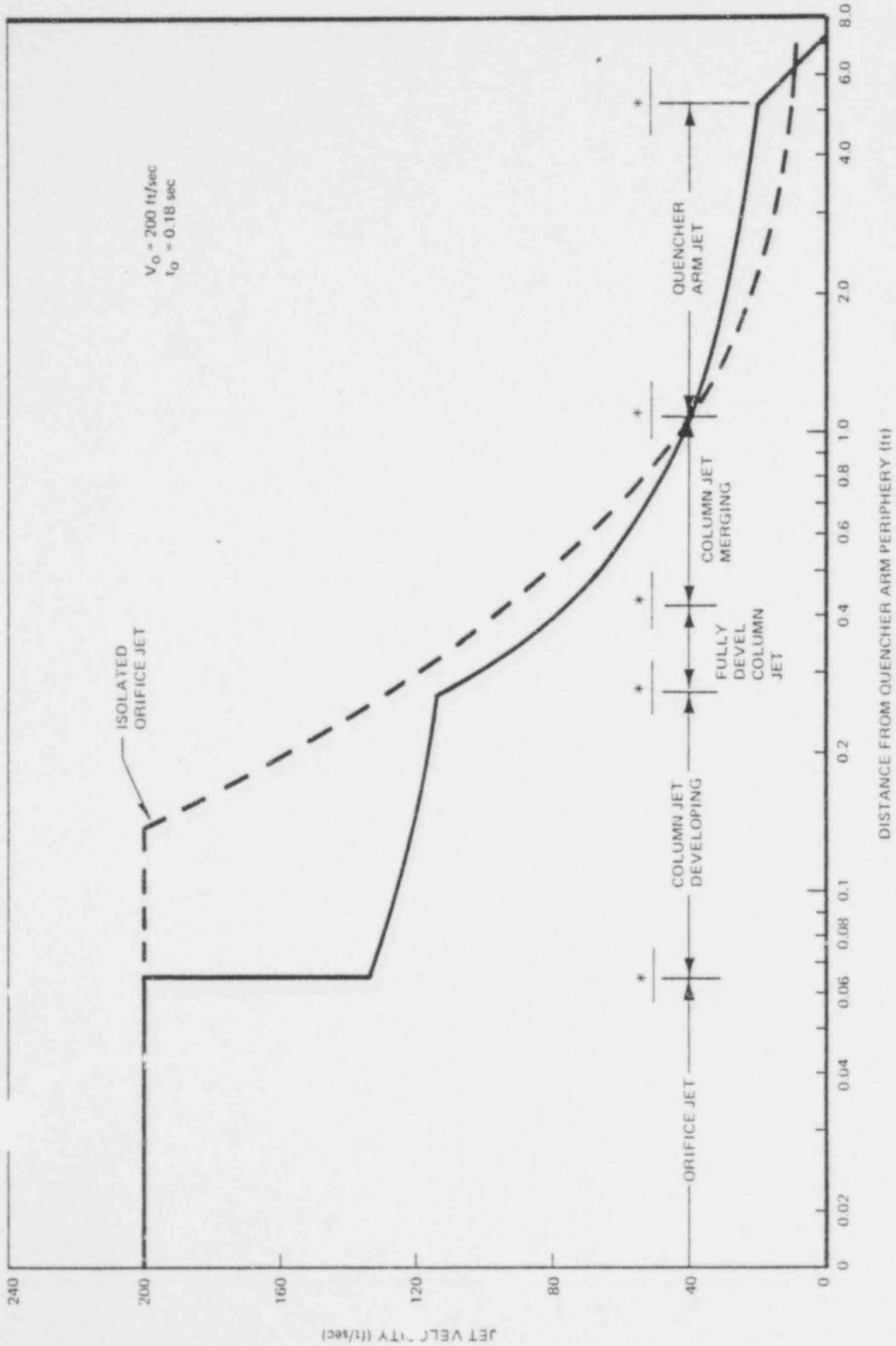


Figure 7. Quencher Jet Velocity vs Downstream Distance

6. END CAP JET

In some designs, the end cap of the quencher arm also contains orifices, and these will form an "end cap jet." The orifices are arranged in    columns separated by    in., with the orifices in any column separated by    inch. There are    orifices in the inner    columns and    in the outer   . The end cap has a spherical radius of curvature of    in., so the divergence angle between any two orifice jets in a column is   ° (rather than the   ° of the quencher arm orifice jets). Since the curvature is spherical, the column jets also diverge geometrically, at an angle of   ° (i.e.,    x 180/10 x π).

Proceeding as before for the quencher arm, the following end cap jet characteristics are derived.

6.1 ORIFICE JETS MERGE TO FORM A COLUMN JET

This occurs during the region where the centerline velocity does not decrease. From Figure 2, for an included angle of   °, and equation 2.5a (with the angle of   ° replaced by   ° and the separation distance  $L_1/2$  equal to    in.), the merging distance works out to be:

$$X_m = \underline{\quad} \text{ in.} = 7.2 r_o \quad (6.1)$$

6.2 COLUMN JETS MERGE TO FORM AN END CAP JET

Each column is analyzed as a two-dimensional rectangular jet to determine where the columns begin to interact. Modifying equation 2.19 to account for the geometric divergence of the columns gives the relation:

$$1.82 \left\{ 0.1038 \left( \frac{X_T - 7.2 r_o}{2.187 r_o} + 0.6 \right) (2.187 \quad) \right\}$$

$$= (1.97''/2 + X_T \sin 5.645/\cos 5.645) \quad (6.2)$$

where the factor  $2.187 r_o$  (corresponding to  $2.107 r_o$  of the quencher jet) is twice the half width of an orifice jet at the location where the orifice jets begin to interact. Solving equation 6.2 gives

$$X_T = 13.4'' = 58.56 r_o \quad (6.3)$$

By comparing this to the quencher arm result (i.e.,  $29.5 r_o$ ), it can be seen that the divergence of the individual column jets of the end cap moves the merging location downstream by about 45 orifice diameters.

The initial velocity of the column jet can be determined by modifying equation 2.12. The calculations are based on eleven orifices per column, rather than an average of eleven and nine, since this gives a higher jet velocity and is thus more conservative. Therefore, conservation of momentum is

$$(11) \pi r_o^2 V_o^2 = \rho V_i^2 \left[ 10 \times 0.78'' + 2 r_o + 7.2 r_o \left( \frac{44.7\pi}{180} \right) \right] \\ * (2.187 r_o) \quad (6.4)$$

or

$$V_i = 0.577 V_o$$

497 120

Using this result, the column jet velocity as a function of distance can be estimated from the previous results for the quencher arm jet. Thus

$$\begin{aligned}
 v &= 0.577 v_o \left[ \frac{60.9}{53.7 + x/r_o} \right]^{1/2} \quad \text{for } 7.2 \leq x/r_o \leq 19.88 \\
 v &= 1.458 v_o \left[ \frac{60.9}{53.7 + x/r_o} \right]^{1/2} / \left[ \frac{x/r_o - 7.2}{2.187} + 0.6 \right]^{1/2}
 \end{aligned}
 \tag{6.5}$$

for  $19.88 \leq x/r_o \leq 68.56$

After the column jets begin to interact at  $x = 68.56 r_o$ , an additional  $38.3 r_o$  is required to merge the columns into one jet, according to equation 2.16.

### 6.3 END CAP JET

The fully merged column jets form a rectangular jet whose initial cross-sectional area is

$$\begin{aligned}
 A &= \left[ 3 * 1.97'' + 2 r_o + 68.56 r_o \left( \frac{33.9\pi}{180} \right) \right] \\
 &\quad * \left[ 10 * 0.78'' + 2 r_o + 68.56 r_o \left( \frac{44.7\pi}{180} \right) \right] \\
 &= 265.38 \text{ in}^2
 \end{aligned}$$

The rectangular jet has an initial velocity determined from momentum considerations:

$$265.38 \rho V_{EC_0}^2 = (4 \times 11) \pi \rho r_0^2 V_0^2$$

or

$$V_{EC_0} = 0.141 V_0 \quad (6.6)$$

Downstream of  $x = 68.56 r_0$ , the end cap jet velocity is further attenuated by the geometric divergence. (The small additional attenuation due to turbulent diffusion is neglected since there are no valid theories or data available to describe it.) Therefore:

$$\begin{aligned} V_Q &= 2.29 V_0 / \left\{ \left[ 6.301 + 0.592 r_0 (x/r_0) \right]^{1/2} \right. \\ &\quad \left. * \left[ 8.191 + 0.780 r_0 (x/r_0) \right]^{1/2} \right\} \\ &= \frac{7.3 V_0}{(54.47 + x/r_0)^{1/2} (53.7 + x/r_0)^{1/2}} \quad (6.7) \end{aligned}$$

## 6.4 TRANSIENT DECAY OF END CAP JET

Proceeding as with equation 3.2, the distance  $X_0$  traveled by the end cap jet up to the time when the orifice flow ceases is determined from:

$$\begin{aligned}
 t_0 = & 7.2 \frac{r_0}{V_0} + \int_{7.2 r_0}^{19.88 r_0} \frac{dx}{0.577 V_0 \left[ 60.9 / (53.7 + x/r_0) \right]^{1/2}} \\
 & + \int_{19.88 r_0}^{68.56 r_0} \frac{\left[ \frac{x/r_0 - 7.2}{2.187} + 0.6 \right]^{1/2} dx}{1.458 V_0 \left[ 60.9 / (53.7 + x/r_0) \right]^{1/2}} \\
 & + \int_{68.56 r_0}^{106.86 r_0} \frac{(x/r_0 - 20.35) dx}{9.26 V_0} \\
 & + \int_{106.86 r_0}^{x_0} \frac{\left[ 54.47 + x/r_0 \right]^{1/2} \left[ 53.70 + x/r_0 \right]^{1/2} dx}{2.29 V_0} \quad (6.8)
 \end{aligned}$$

In the last term, the factors  $x/r_0$ 's are predominant for  $x > 106.86 r_0$ , so the entire term is simplified to

$$\int_{106.86 r_0}^{x_0} \frac{(54.09 + x/r_0) dx}{17.3 V_0}$$

The approximate integrand is in error by only about 0.3% at  $x = 106.86 r_0$ , and the error decreases as  $x$  increases. The approximate integrand, moreover,

has the virtue that it eliminates the need to solve a transcendental equation for  $X_o$  in the results. With this simplification, equation (6.8) gives

$$t_o v_o / r_o = 7.2 + 23.08 + 175.66 + 276.61 - 748.70 + \frac{(54.09 + x/r_o)^2}{2(17.3)} \quad (6.9)$$

Thus,

$$X_o = \left\{ 5.882 \left( \frac{t_o v_o}{r_o} + 266.15 \right)^{1/2} - 54.09 \right\} r_o \quad (6.10)$$

which is valid for  $t_o v_o / r_o \geq 482.6$

The jet velocity at the end of the orifice flow period is

$$\frac{v_{Q_o}}{v_o} = \frac{17.3}{\left[ 54.47 + 5.882 \left( \frac{t_o v_o}{r_o} + 266.15 \right)^{1/2} - 54.09 \right]^{1/2} \left[ 53.7 + 5.882 \left( \frac{t_o v_o}{r_o} + 266.15 \right)^{1/2} - 54.09 \right]^{1/2}}$$

$$\approx \frac{17.3}{5.882 \left( \frac{t_o v_o}{r_o} + 266.15 \right)^{1/2}} = \frac{2.941}{\left( \frac{t_o v_o}{r_o} + 266.15 \right)^{1/2}} \quad (6.11)$$

and the total penetration distance is

$$X_T = X_o + \frac{1}{2} v_{Q_o} t_o$$

$$\frac{X_T}{r_o} = \frac{X_o}{r_o} + \frac{1}{2} \left( \frac{v_{Q_o}}{v_o} \right) \left( \frac{t_o v_o}{r_o} \right)$$

7. SUMMARY OF RESULTS FOR END CAP JET

The symbols used are the same as for the quencher arm jet.

- $0 \leq x \leq 7.2 r_o$  (orifice jet)

$$V = V_o$$

$$r_{1/2} = r_o [1 + 0.013 x/r_o]$$

- $7.2 r_o \leq x \leq 68.56 r_o$  (column jets)

$$V = 0.577 V_o [60.9/(53.7 + x/r_o)]^{1/2}$$

$$W = 0.780 r_o (53.7 + x/r_o)$$

$$2 y_{1/2} = 2.187 r_o [1 + 0.0259 (x/r_o - 7.2)]$$

for  $7.2 \leq x/r_o \leq 19.88$ , and

$$V = 1.458 V_o [60.9/(53.7 + x/r_o)]^{1/2} / \left[ \frac{x/r_o - 7.2}{2.187} + 0.6 \right]^{1/2}$$

$$W = 0.780 r_o (53.7 + x/r_o)$$

$$2 y_{1/2} = 0.454 r_o \left( \frac{x/r_o - 7.2}{2.187} + 0.6 \right)$$

for  $19.88 \leq x/r_o \leq 68.56$

- $68.56 r_o \leq x \leq 106.86 r_o$  (column jets merging)

$$V = 9.26 V_o / (x/r_o - 20.35)$$

$$W = 0.780 r_o (53.7 + x/r_o)$$

$$B = 0.592 r_o [54.4 + x/r_o]$$

$$\bullet \quad \frac{106.86 r_o \leq x \leq \left\{ 5.882 \left[ \frac{t_o V_o}{r_o} + 266.15 \right]^{1/2} - 54.09 \right\} r_o}{17.3 V_o}$$

$$V = \frac{17.3 V_o}{\left[ 54.47 + (x/r_o) \right]^{1/2} \left[ 53.7 + (x/r_o) \right]^{1/2}}$$

$$W = 0.780 r_o (53.7 + x/r_o)$$

$$B = 0.592 r_o (54.44 + x/r_o)$$

$$\bullet \quad \frac{\left\{ 5.882 \left[ \frac{t_o V_o}{r_o} + 266.15 \right]^{1/2} - 54.09 \right\} r_o \leq x \leq X_{TOTAL}}{17.3 V_o}$$

$$V = V_{Q_o} \left[ \frac{V_{Q_o} t_o - 2(x - X_o)}{V_{Q_o} t_o} \right]$$

$$W = 0.780 r_o (53.7 + x/r_o)$$

$$B = 0.592 r_o (54.44 + x/r_o)$$

where

$$V_{Q_o} = \frac{2.941 V_o}{\left( \frac{t_o V_o}{r_o} + 266.15 \right)^{1/2}}$$

$$X_o = \left\{ 5.882 \left( \frac{t_o V_o}{r_o} + 266.15 \right)^{1/2} - 54.09 \right\} r_o$$

$$X_{TOTAL} = X_o + \frac{1}{2} V_{Q_o} t_o$$

8. NUMERICAL EXAMPLE FOR END CAP JET

Typical parameters are

$$V_0 = 200 \text{ ft/sec}$$

$$t_0 = 0.18 \text{ sec}$$

$$r_0 = \underline{\quad * \quad} \text{ in.}$$

Using these data, the jet has penetrated a distance

$$X_0 = 238.6 r_0 = \underline{\quad * \quad} \text{ ft}$$

and has a velocity

$$V_{Q_0} = 0.0591 V_0 = 11.82 \text{ ft/sec}$$

after a time period  $t_0 = 0.18 \text{ sec}$ . The total penetration of the jet is

$$X_T = 304.1 r_0 = \underline{\quad * \quad} \text{ ft}$$

Compared to the quencher arm jet, these substantially smaller values for the penetration distance and velocity show the effect of the three-dimensional attenuation of the end cap jet.

9. FOP PREDICTIONS

If the structure is fully engulfed within the jet boundary, the drag load on structure is calculated as follows:

$$F = C_D \frac{\rho}{2g_c} A_x V_N^2 \quad (9.1)$$

where

$F$  = force normal to structure axis ( $lb_f$ )

$C_D$  = standard drag coefficient

$\rho$  = density of water ( $62.4 \text{ lbm/ft}^3$ )

$g_c$  = gravitational constant ( $32.2 \text{ lb}_m \text{ ft/lb}_f\text{-sec}^2$ )

$A_x$  = projected structure area engulfed by the jet ( $\text{ft}^2$ )

$V_N$  = maximum jet velocity normal to structure axis ( $\text{ft/sec}$ )

If a structure fully or partially intercepts the jet, the following equation should be used. The equation is derived based on momentum stoppage of a jet.

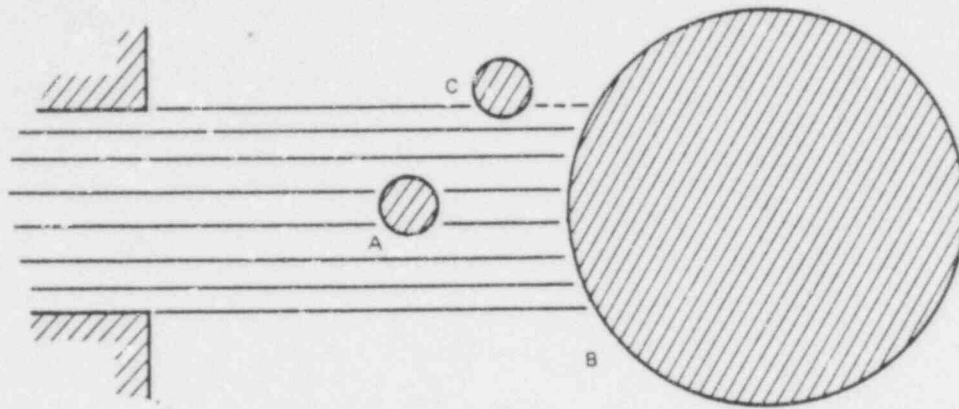
$$F = K \frac{\rho}{2g_c} A_I V_N^2 \quad (9.2)$$

where

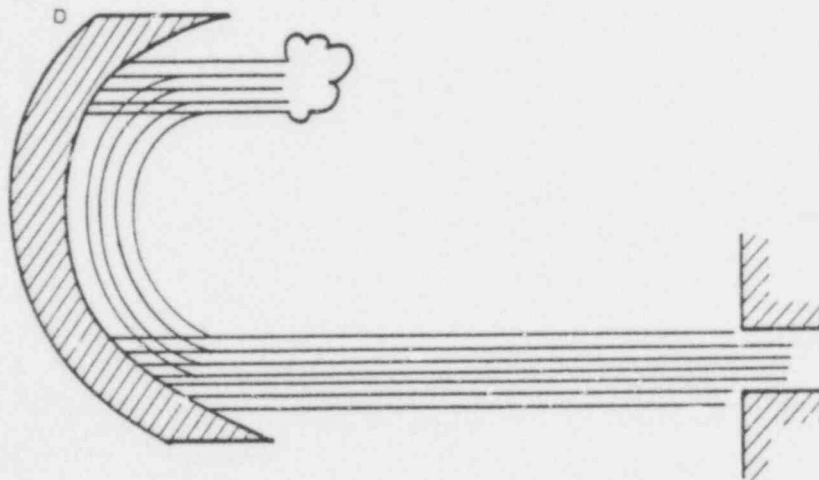
$A_I$  = intercepted jet area normal to the jet direction ( $\text{ft}^2$ )

$K = 2$ , jet momentum stoppage without reflection

$= 4$ , jet turns back away from the structure (e.g., a concaved shaped structure) (See Figure 8).



STRUCTURE A: FULLY SUBMERGED, USE  $C_D$  AND EQUATION 9.1  
 B: FULLY INTERCEPTS JET, USE K AND EQUATION 9.2  
 C: PARTIALLY INTERCEPTS JET, USE K AND EQUATION 9.2



STRUCTURE D: TURNS JET BACK ON ITSELF, USE K AND EQUATION 9.2

Figure 8. Possible Structure/Jet Interactions

The drag load calculated here is conservatively assumed to apply on the structure for a period of  $2 t_0$ .

10. REFERENCES

1. H. Schlichting, BOUNDARY LAYER THEORY, 4th Edition, McGraw-Hill Book Co., 1960.
2. P. Witze, "Centerline Velocity Decay of Compressible Free Jets," *AIAA J.*, 12, pp 407-408, April 1974.
3. G. Kleinstein, "Mixing in Turbulent Axially Symmetric Jets," *AIAA J. Spacecraft/Rockets*, 1, pp 403-408, July/August 1964.
4. A. J. Wheeler, "Analytical Model For Computing Transient Pressures and Forces in the Safety/Relief Valve Discharge Line," NEDE 23749P.
5. J. W. Gaunter, J. N. B. Livingood, and P. Hrycak, "Survey of Literature on Flow Characteristics of a Single Turbulent Jet Impinging on a Flat Plate," NASA TN D-5652, February 1970.
6. A. A. Sfeir, "The Velocity and Temperature Fields of Rectangular Jets," *Int. J. Heat/Mass Transfer*, 19, pp 1289-1297, 1976.
7. S. Beltaos, "Oblique Impingement of Plane Turbulent Jets," *Proc. ASCE, J. Hydraulics Div.*, 102, pp 1177-1192, September 1976.
8. S. Beltaos and N. Rajaratnam, "Impinging Circular Turbulent Jets," *Proc. ASCE, J. Hydraulics Div.*, 100, pp 1313-1328, October 1974.
9. P. Hrycak, D. T. Lee, J. W. Gauntner and J. N. B. Livingood, "Experimental Flow Characteristics of a Single-Turbulent Jet Impinging on a Flat Plate," NASA TN D-5690, March 1970.
10. F. T. Dodge and R. E. Ricker, "Flow of Liquid Jets Through Closely Woven Screens," *AIAA J. Spacecraft/Rockets*, 15, pp 213-218, July-August 1978.

APPENDIX A

MODIFIED ANALYTICAL MODEL  
FOR  
T-QUENCHER WATER JET LOADS  
ON  
SUBMERGED STRUCTURES

Prepared by:  
NUCLEAR SERVICES CORPORATION  
under

P. O. #205-G7-F56

Prepared by:

K. H. Chu

January 23, 1979

TABLE OF CONTENTS

	<u>Page</u>
A1. INTRODUCTION	A-1
A2. DYNAMICS OF THE QUENCHER ARM JET	A-3
A3. DYNAMICS OF THE END CAP JET	A-18
A4. DETERMINATION OF $v_{o,j}$ AND $\tau_{o,j}$	A-21

A1. INTRODUCTION

In the T-quencher water jet model, it is assumed that the hole pattern is uniform and the orifice water velocity  $V_0$  and the time at which water flowing through the orifice  $t_0$  are identical for each hole. The modified T-quencher water jet model relaxes the above assumptions by dividing the quencher arm into six sections (seven for quencher arm with end cap holes) as shown in Figure A.1. Each section has a different but uniform hole pattern. The values of  $V_0$  and  $t_0$  for the orifices in the same section are assumed to be identical.

The velocities for jets from each section of the arm are derived with the method similar to that in the T-quencher water jet model. The method can be summarized as follows: (a) steady-state submerged-jet theories are used for the orifice jets, column jets, and quencher arm jets; (b) after the flow of liquid through the orifices has stopped, the velocity and the penetration distance of the quencher jet are determined with the aid of scale-model test data.

General Electric  
Company Proprietary

Figure A-1. Jet Sections Along the Quencher Arm on Torus Plan View  
(G.E. Company Proprietary)

A2. DYNAMICS OF THE QUENCHER ARM JET

In the modified T-quencher water jet model, it is assumed that there is no interaction between the jets from different sections of the quencher arms. The dynamics of the jets from each section are deduced following the analyses in Sections 2 and 3. A summary of the results is shown in Tables A-1 and A-2.

## A2.1 ORIFICE JETS

Following Equations (2.1b) and (2.4) in Section 2.1, the general results for the orifice jets from the arm are as follows:

$$\frac{V_j}{V_{o,j}} = 1 \quad j = 1, 2, 3, \dots, 6$$

$$\frac{r_{1/2,j}}{r_o} = 1 + 0.013 \frac{x}{r_o} \quad j = 1, 2, 3, \dots, 6$$

for

$$0 < \frac{x}{r_o} \leq 4.1$$

where

- $V_j$  = Jet velocity at a distance "x" downstream of the orifice
- $V_{o,j}$  = Jet velocity at the orifice
- $r_{1/2,j}$  = Half-width of the orifice jet
- $r_o$  = Orifice radius =        \* in.

where the subscript "j" represents the section number in the arm.

Table A-1

SUMMARY OF DIMENSIONLESS VELOCITY PROFILES ( $V^* = V/V_o$ ) FOR THE T-QUENCHER ARM JETS

Range	Sections 1 and 2	Section 3	Section 4	Sections 5 and 6
$0 \leq X^* \leq 4.1$	1	1	1	1
$4.1 \leq X^* \leq 16.3$	$0.71 \left( \frac{47.27}{43.17 + X^*} \right)^{1/2}$	$0.68 \left( \frac{40.20}{36.10 + X^*} \right)^{1/2}$	$0.67 \left( \frac{38.79}{34.69 + X^*} \right)^{1/2}$	$0.67 \left( \frac{45.3}{41.2 + X^*} \right)^{1/2}$
$16.3 \leq X^* \leq 29.5$	$\frac{1.79 \left( \frac{47.27}{43.17 + X^*} \right)^{1/2}}{\left( \frac{X^* - 4.1}{2.107} + 0.6 \right)^{1/2}}$	$\frac{1.71 \left( \frac{40.20}{36.10 + X^*} \right)^{1/2}}{\left( \frac{X^* - 4.1}{2.107} + 0.6 \right)^{1/2}}$	$\frac{1.70 \left( \frac{38.79}{34.69 + X^*} \right)^{1/2}}{\left( \frac{X^* - 4.1}{2.107} + 0.6 \right)^{1/2}}$	$\frac{1.70 \left( \frac{45.30}{41.2 + X^*} \right)^{1/2}}{\left( \frac{X^* - 4.1}{2.107} + 0.6 \right)^{1/2}}$
$29.5 \leq X^* \leq 67.8$	$\frac{18.95}{X^* + 17.17}$	$\frac{16.90}{X^* + 15.44}$	$\frac{16.44}{X^* + 14.81}$	$\frac{17.62}{X^* + 16.50}$
$67.8 \leq X^* \leq X^*_{oj}$	$\frac{2.35}{(X^* + 43.17)^{1/2}}$	$\frac{2.07}{(X^* + 36.10)^{1/2}}$	$\frac{2.01}{(X^* + 34.69)^{1/2}}$	$\frac{2.19}{(X^* + 41.20)^{1/2}}$
$X^*_{oi} \leq X^* \leq X^*_{tj}$	$V^*_{Q_{oj}} \left[ 1 - \frac{2}{V^*_{Q_{oj}} P_j} (X^* - X^*_{oj}) \right]^{1/2}$			
$V^*_{Q_{oj}}$	$\frac{1.54}{(P_j + 146.69)^{1/3}}$	$\frac{1.42}{(P_j + 143.54)^{1/3}}$	$\frac{1.39}{(P_j + 143.32)^{1/3}}$	$\frac{1.47}{(P_j + 153.52)^{1/3}}$

Table A-1

SUMMARY OF DIMENSIONLESS VELOCITY PROFILES FOR THE T-QUENCHER ARM JETS (Continued)

Range	Sections 1 and 2	Section 3	Section 4	Sections 5 and 6
$X_{oi}^*$	$2.31 (P_j + 149.69)^{2/3}$	$2.13 (P_j + 143.54)^{2/3}$	$2.08 (P_j + 143.32)^{2/3}$	$2.21 (P_j + 153.52)^{2/3}$
	-43.17	-36.10	-34.69	-41.0
$X_{tj}^*$	←----- $X_{oj}^* + \frac{1}{2} V_{oj}^* P_j$ -----→			
$P_j$	←----- $\frac{V_{oj} t_{oj}}{r_o}$ -----→			
$X^*$	←----- $\frac{x}{r_o}$ -----→			

A-5

NEDO-25090

497 137

Table A-2

SUMMARY OF DIMENSIONLESS JET WIDTHS AND HEIGHTS OF THE T-QUENCHER ARM JETS

$$B_j^* = B/r_o$$

<u>Range</u>	<u>Sections 1 and 2</u>	<u>Section 3</u>	<u>Section 4</u>	<u>Sections 5 and 6</u>
$0 \leq X^* \leq 4.1$	←----- $2(1 + 0.013X^*)$ -----→			
$4.1 \leq X^* \leq 16.3$	←----- $2.107 [1 + 0.027(X^* - 4.1)]$ -----→			
$16.3 \leq X^* \leq 29.5$	←----- $0.437 \left[ \frac{X^* - 4.1}{2.107} + 0.6 \right]$ -----→			
$29.5 \leq X^* \leq X_{tj}^*$	←----- $70.54$ -----→			

$$W_j^* = W/2r_o$$

<u>Range</u>	<u>Sections 1 and 2</u>	<u>Section 3</u>	<u>Section 4</u>	<u>Sections 5 and 6</u>
$0 \leq X^* \leq 4.1$	$1 + 0.013 X^*$			
$4.1 \leq X^* \leq X_{tj}$	$0.095(43.17 + X^*)$	$0.285(36.10 + X^*)$	$0.47(36.49 + X^*)$	$0.47(42.1 + X^*)$

A-6

NEDO-25090

497 138

Table A-3  
SUMMARY OF DIMENSIONLESS END CAP JET WIDTHS, HEIGHTS, AND VELOCITIES

Region	$\frac{V/V_0}{\dots}$	$\frac{M/2r_0}{\dots}$	$\frac{H/r_0}{\dots}$
$0 - \frac{x}{r_0} - 7.2$	1	$(1 + 0.013 \frac{x}{r_0})$	$2 \left( 1 + 0.013 \frac{x}{r_0} \right)$
$7.2 - \frac{x}{r_0} - 19.88$	$0.571 \left( \frac{60.90}{53.70 + \frac{x}{r_0}} \right)^{1/2}$	$0.19 \left( 53.7 + \frac{x}{r_0} \right)$	$2.187 \left[ 1 + 0.0259 \left( \frac{x}{r_0} - 7.2 \right) \right]$
$19.88 - \frac{x}{r_0} - 68.56$	$1.438 \left( \frac{60.90}{53.70 + \frac{x}{r_0}} \right)^{1/2}$ $\frac{\left( \frac{x}{r_0} - 7.2 \right)}{\left( \frac{x}{r_0} - 7.2 \right)} + 0.6$	$0.19 \left( 53.7 + \frac{x}{r_0} \right)$	$0.454 \left( \frac{x}{r_0} - 7.2 \right) + 0.48$
$68.56 - \frac{x}{r_0} - 106.86$	$\frac{9.26}{\frac{x}{r_0} - 20.35}$	$0.19 \left( 53.7 + \frac{x}{r_0} \right)$	$0.592 \left( 54.44 + \frac{x}{r_0} \right)$
$106.86 - \frac{x}{r_0} - \frac{r_u}{r_0}$	$\frac{12.3}{\left( 54.47 + \frac{x}{r_0} \right)^{1/2}} \left( 53.7 + \frac{x}{r_0} \right)^{1/2}$	$0.19 \left( 53.7 + \frac{x}{r_0} \right)$	$0.592 \left( 54.44 + \frac{x}{r_0} \right)$
$\frac{x}{r_0} - \frac{x}{r_0} - \frac{r_u}{r_0} - \frac{r_u}{r_0}$	$\frac{V_0}{V_0} \left[ 1 - \frac{V_0}{V_0} \frac{r_0}{V_0} \left( \frac{x}{r_0} - \frac{r_u}{r_0} \right) \right]$	$0.19 \left( 53.7 + \frac{x}{r_0} \right)$	$0.592 \left( 54.44 + \frac{x}{r_0} \right)$
$\frac{x}{r_0} - \left\{ 3.882 \left( \frac{r_u}{r_0} - 266.15 \right)^{1/2} - 54.09 \right\}$			
$\frac{x}{r_0} - \frac{r_u}{r_0} + \frac{1}{2} \frac{V_0}{V_0} \frac{r_0}{r_0}$			
$\frac{V_0}{V_0} = \frac{2.94}{\left( \frac{r_u}{r_0} + 266.15 \right)^{1/2}}$			

## A2.2 COLUMN JETS - ISOLATED COLUMN REGION

Following Equations (2.10) and (2.11) in Section 2.2, the general results for the column jets are as follows:

For  $4.1 \leq x/r_o \leq 16.3$

$$\frac{V_j}{V_{i,j}} = \left[ \frac{(n_j-1) L_1 + 2r_o + 4.1 r_o \theta_j}{(n_j-1) L_1 + 2r_o + x \theta_j} \right]^{\frac{1}{2}} \quad j = 1, 2, \dots, 6$$

$$\frac{W_j}{r_o} = (n_j-1) \frac{L_1}{r_o} + 2 + \frac{x}{r_o} \theta_j \quad j = 1, 2, \dots, 6$$

$$\frac{2y_{1,2,j}}{r_o} = 2.107 \left[ 1 + 0.027 \left( \frac{x}{r_o} - 4.1 \right) \right] \quad j = 1, 2, \dots, 6$$

For  $16.3 \leq x/r_o \leq 29.5$

$$\frac{V_j}{V_{i,j}} = \frac{2.53 \left[ \frac{(n_j-1) L_1 + 2r_o + 4.1 r_o \theta_j}{(n_j-1) L_1 + 2r_o + x \theta_j} \right]^{\frac{1}{2}}}{\left( \frac{x/r_o - 4.1}{2.107} + 0.6 \right)^{1/2}} \quad j = 1, 2, \dots, 6$$

$$\frac{W_j}{r_o} = (n_j-1) \frac{L_1}{r_o} + 2 + \frac{x}{r_o} \theta_j \quad j = 1, 2, \dots, 6$$

$$\frac{2y_{1,2,j}}{r_o} = 0.44 \left( \frac{x/r_o - 4.1}{2.107} + 0.6 \right) \quad j = 1, 2, \dots, 6$$

where

$$V_{i,j} = V_{o,j} \left[ \frac{n_j \pi r_o}{2.107 [(n_j - 1) L_1 + 2r_o + 4.1r_o \theta_j]} \right]^{1/2}$$

$n_j$  = The number of orifice in a row in Section  $j$

$L_1$  = Spacing between the orifice in the same row

= \* in.

$$\theta_j = \begin{cases} \frac{(n_j - 1) 5.4\pi}{180} & j = 1, 2, 3, 4 \\ 54 \frac{\pi}{180} & j = 5, 6 \end{cases}$$

$W_j$  = Height of the column jet

$y_{1/2,j}$  = Half-width of the column jet in Section  $j$

Based on the above general formulas, the detailed governing equations for the jets from each section of the arm can be obtained as follows:

For  $4.1 \leq x/r_o \leq 16.3$

$$\frac{V_j}{V_{o,j}} = 0.71 \left[ \frac{47.27}{43.17 + \frac{x}{r_o}} \right]^{1/2} \quad j = 1, 2$$

$$\frac{V_j}{V_{o,j}} = 0.68 \left[ \frac{40.20}{36.10 + \frac{x}{r_o}} \right]^{1/2} \quad j = 3$$

$$\frac{V_j}{V_{o,j}} = 0.67 \left[ \frac{38.79}{34.69 + \frac{x}{r_o}} \right]^{1/2} \quad j = 4$$

$$\frac{V_j}{V_{o,j}} = 0.67 \left[ \frac{45.30}{41.20 + \frac{x}{r_o}} \right]^{1/2} \quad j = 5, 6$$

$$\frac{W_j}{r_o} = 0.19 \left( 43.17 + \frac{x}{r_o} \right) \quad j = 1, 2$$

$$\frac{W_j}{r_o} = 0.57 \left( 36.10 + \frac{x}{r_o} \right) \quad j = 3$$

$$\frac{W_j}{r_o} = 0.94 \left( 34.69 + \frac{x}{r_o} \right) \quad j = 4$$

$$\frac{W_j}{r_o} = 0.94 \left( 41.20 + \frac{x}{r_o} \right) \quad j = 5, 6$$

$$\frac{2Y_{1,2,j}}{r_o} = 2.107 \left( 1 + 0.027 \left( \frac{x}{r_o} - 4.1 \right) \right) \quad j = 1, 2, \dots, 6$$

For  $16.3 \leq x/r_o \leq 29.5$

$$\frac{V_j}{V_{o,j}} = \frac{1.79 \left( \frac{47.27}{43.1 + x/r_o} \right)^{1/2}}{\left( \frac{x}{r_o} - 4.1 \right)^{1/2} \left( \frac{2.107}{2.107} + 0.6 \right)} \quad j = 1, 2$$

$$\frac{v_j}{v_{o,j}} = \frac{1.71 \left( \frac{40.20}{36.10 + x/r_o} \right)}{\left( \frac{\frac{x}{r_o} - 4.1}{2.107} + 0.6 \right)^{1/2}} \quad j = 3$$

$$\frac{v_j}{v_{o,j}} = \frac{1.70 \left( \frac{38.79}{34.69 + x/r_o} \right)^{1/2}}{\left( \frac{\frac{x}{r_o} - 4.1}{2.107} + 0.6 \right)^{1/2}} \quad j = 4$$

$$\frac{v_j}{v_{o,j}} = \frac{1.70 \left( \frac{45.30}{41.20 + x/r_o} \right)^{1/2}}{\left( \frac{\frac{x}{r_o} - 4.1}{2.107} + 0.6 \right)^{1/2}} \quad j = 5, 6$$

$$\frac{w_j}{r_o} = 0.19 \left( 43.17 + \frac{x}{r_o} \right) \quad j = 1, 2$$

$$\frac{w_j}{r_o} = 0.57 \left( 36.10 + \frac{x}{r_o} \right) \quad j = 3$$

$$\frac{w_j}{r_o} = 0.94 \left( 34.69 + \frac{x}{r_o} \right) \quad j = 4$$

$$\frac{w_j}{r_o} = 0.94 \left( 41.20 + \frac{x}{r_o} \right) \quad j = 5, 6$$

$$\frac{2y_{1,2,j}}{r_o} = 0.44 \left( \frac{\frac{x}{r_o} - 4.1}{2.107} + 0.6 \right) \quad j = 1, 2, \dots, 6$$

## A2.3 COLUMN JETS - MERGED COLUMN REGION

Following Equation (2.18) in Section 2.2, the general results are as follows:

For  $29.5 \leq x/r \leq 67.8$

$$\frac{V_j}{V_{o,j}} = \frac{a_j}{x/r_o + b_j} \quad j = 1, 2, \dots, 6$$

$$\frac{W_j}{r_o} = (n_j - 1) \frac{L_1}{r_o} + 2 + \frac{x}{r_o} \theta_j \quad j = 1, 2, \dots, 6$$

$$\frac{B_j}{r_o} = \frac{(m_j - 1) L_2}{r_o} \quad j = 1, 2, \dots, 6$$

where

$m_j$  = Number of row in section  $j$

$L_2$  = Spacing between the rows

= \* in.

$B_j$  = Width of the merged column jet in Section  $j$

$a_j$  and  $b_j$  are constants determined by the following equations:

$$\frac{a_j}{29.5 + b_j} = 0.49 \left[ \frac{n_j \pi r_o}{(n_j - 1) L_1 + 2r_o + 29.5 r_o \theta_j} \right]^{1/2}$$

$$\frac{a_j}{67.8 + b_j} = \left\{ \frac{m_j n_j \pi r_o}{[(m_j - 1) L_2 + 2r_o] [(n_j - 1) L_1 + 2r_o + 67.8 r_o \theta_j]} \right\}^{1/2}$$

Based on the above general formula, the detailed governing equations for the jets from each section of the arm can be obtained as follows:

For  $29.5 \leq x/r_o \leq 67.8$

$$\frac{V_j}{V_{o,j}} = \frac{18.95}{x/r_o + 17.17} \quad j = 1, 2$$

$$\frac{V_j}{V_{o,j}} = \frac{16.90}{15.44 + x/r_o} \quad j = 3$$

$$\frac{V_j}{V_{o,j}} = \frac{16.44}{14.81 + x/r_o} \quad j = 4$$

$$\frac{V_j}{V_{o,j}} = \frac{17.62}{16.50 + x/r_o} \quad j = 5, 6$$

$$\frac{W_j}{r_o} = 0.19 \left( 43.17 + \frac{x}{r_o} \right) \quad j = 1, 2$$

$$\frac{W_j}{r_o} = 0.57 \left( 36.10 + \frac{x}{r_o} \right) \quad j = 3$$

$$\frac{W_j}{r_o} = 0.94 \left( 34.69 + \frac{x}{r_o} \right) \quad j = 4$$

$$\frac{W_j}{r_o} = 0.94 \left( 41.20 + \frac{x}{r_o} \right) \quad j = 5, 6$$

$$\frac{B_j}{r_o} = 70.54 \quad j = 1, 2, \dots, 6$$

## A2.4 QUENCHER ARM JETS

Following Equation (2.1) in Section 2.2, the general quencher arm jet velocity can be expressed as

For  $67.8 \leq x/r_o \leq x_{o,j}/r_o$

$$\frac{v_j}{v_{o,j}} = \left\{ \frac{m_j n_j \pi r_o^2}{[(m_j-1) L_2 + 2r_o][(n_j-1) L_1 + 2r_o + x_{o,j}]} \right\}^{1/2} \quad j = 1, 2, \dots, 6$$

where  $x_{o,j}$  is the quencher jet penetration at  $t = t_{o,j}$  and  $t_{o,j}$  is the time at which water flow through orifices ceases in Section  $j$ . The expressions for the jet width and height of the quencher arm jet are the same as those in Section A2.3.

Following Equation (3.2) in Section 3, the general expression for  $x_{o,j}$  can be obtained as follows:

$$\frac{t_{o,j} v_{o,j}}{r_o} = \int_0^{x_{o,j}/r_o} \frac{v_j}{v_{o,j}} d\left(\frac{x}{r_o}\right) \quad j = 1, 2, \dots, 6$$

By substituting the corresponding expression of  $v_j/v_{o,j}$  and carrying out the integration,  $x_{o,j}/r_o$  can be obtained as a function of the parameter

$$P_j = \frac{t_{o,j} v_{o,j}}{r_o}$$

Based on the above general formula, the detailed expressions of quencher arm jet velocity and  $x_{o,j}$  from each section of the arm can be obtained as follows:

For  $67.8 \leq x/r_o \leq x_{o,j}/r_o$

$$\frac{V_j}{V_{o,j}} = \frac{2.348}{(43.17 + x/r_o)^{1/2}} \quad j = 1,2$$

$$\frac{V_j}{V_{o,j}} = \frac{2.071}{(36.10 + x/r_o)^{1/2}} \quad j = 3$$

$$\frac{V_j}{V_{o,j}} = \frac{2.011}{(34.69 + x/r_o)^{1/2}} \quad j = 4$$

$$\frac{V_j}{V_{o,j}} = \frac{2.186}{(41.20 + x/r_o)^{1/2}} \quad j = 5,6$$

and

$$\frac{x_{o,j}}{r_o} = 2.31 (P_j + 149.69)^{2/3} - 43.17 \quad j = 1,2$$

$$\frac{x_{o,j}}{r_o} = 2.13 (P_j + 143.54)^{2/3} - 36.10 \quad j = 3$$

$$\frac{x_{o,j}}{r_o} = 2.08 (P_j + 143.32)^{2/3} - 34.69 \quad j = 4$$

$$\frac{x_{o,j}}{r_o} = 2.21 (P_j + 153.52)^{2/3} - 41.20 \quad j = 5,6$$

where

$$P_j = \frac{t_{o,j} V_{o,j}}{r_o}$$

## A2.5 TRANSIENT DECAY OF QUENCHER ARM JETS

Following Equation (3.23) in Section 3, the general velocity-distance relation during the transient decay can be derived as follows

For  $x_{o,j}/r_o \leq x/r_o \leq x_{t,j}/r_o$

$$\frac{V_j}{V_{o,j}} = \frac{V_{Q_{o,j}}}{V_{o,j}} \left[ 1 - \frac{2}{P_j} \frac{V_{o,j}}{V_{Q_{o,j}}} \left( \frac{x}{r_o} - \frac{x_{o,j}}{r_o} \right) \right]^{1/2} \quad j = 1, 2, \dots, 6$$

where  $x_{t,j}$  is the total penetration of quencher jet from Section  $j$  and from Equation (3.2) in Section 3, it is expressed as:

$$\frac{x_{t,j}}{r_o} = \frac{x_{o,j}}{r_o} + \frac{1}{2} \left( \frac{V_{Q_{o,j}}}{V_{o,j}} \right) P_j \quad j = 1, 2, \dots, 6$$

$V_{Q_{o,j}}$  is the value of quencher arm jet velocity at  $t = t_{o,j}$  (or at  $x = x_{o,j}$ ) and it can be determined by substituting  $x = x_{o,j}$  into the expression of  $V_j/V_{o,j}$  in the quencher arm jet.

The expressions for the jet width and height of the decaying quencher arm jet are the same as those in Section A2.3.

Based on the above general formulas, the detailed expressions of decaying quencher arm jet velocity,  $V_{Q_{o,j}}$ , and total jet penetration can be obtained as follows:

For  $x_{o,j}/r_o \leq x/r_o \leq x_{t,j}/r_o$

$$\frac{V_j}{V_{o,j}} = \frac{V_{Q_{o,j}}}{V_{o,j}} \left[ 1 - \frac{2}{P_j} \frac{V_{o,j}}{V_{Q_{o,j}}} \left( \frac{x}{r_o} - \frac{x_{o,j}}{r_o} \right) \right]^{1/2} \quad j = 1, 2, \dots, 6$$

497 148

where

$$\frac{v_{Q_o,j}}{v_{o,j}} = \frac{1.54}{(P_j + 149.69)^{1/3}} \quad j = 1,2$$

$$\frac{v_{Q_o,j}}{v_{o,j}} = \frac{1.42}{(P_j + 143.54)^{1/3}} \quad j = 3$$

$$\frac{v_{Q_o,j}}{v_{o,j}} = \frac{1.39}{(P_j + 143.32)^{1/3}} \quad j = 4$$

$$\frac{v_{Q_o,j}}{v_{o,j}} = \frac{1.47}{(P_j + 153.52)^{1/3}} \quad j = 5,6$$

and

$$\frac{x_{t,j}}{r_o} = \frac{x_{o,j}}{r_o} + \frac{1}{2} \left( \frac{v_{Q_o,j}}{v_{o,j}} \right) P_j \quad j = 1,2,\dots,6$$

A3. DYNAMICS OF THE END CAP JET

By following the analyses in Section 6 and assuming that there is no interaction between the jets from different sections of the quencher arm, the following results are obtained:

Orifice Jets ( $0 \leq x/r_o \leq 7.2$ )

$$\frac{V_j}{V_{o,j}} = 1 \quad j = 7$$

$$\frac{r_{1/2,j}}{r_o} = 1 + 0.013 \frac{x}{r_o} \quad j = 7$$

Column Jets - Isolated Column Region ( $7.2 \leq x/r_o \leq 68.56$ )

For  $7.2 \leq x/r_o \leq 19.88$

$$\frac{V_j}{V_{o,j}} = 0.577 \left( \frac{60.90}{53.70 + x/r_o} \right)^{1/2} \quad j = 7$$

$$\frac{W_j}{r_o} = 0.78 \left( 53.70 + \frac{x}{r_o} \right) \quad j = 7$$

$$\frac{2Y_{1/2,j}}{r_o} = 2.187 \left[ 1 + 0.026 \left( \frac{x}{r_o} - 7.2 \right) \right] \quad j = 7$$

For  $19.88 \leq x/r_o \leq 68.56$

$$\frac{V_j}{V_{o,j}} = \frac{1.458 \left( \frac{60.90}{53.79 + x/r_o} \right)^{1/2}}{\left( \frac{x/r_o - 7.2}{2.187} + 0.6 \right)^{1/2}} \quad j = 7$$

$$\frac{W_j}{r_o} = 0.78 \left( 53.7 + \frac{x}{r_o} \right) \quad j = 7$$

$$\frac{2Y_{1/2,j}}{r_o} = 0.454 \left( \frac{x/r_o - 7.2}{2.187} + 0.6 \right) \quad j = 7$$

Column Jets - Merged Column Region ( $68.56 \leq x/r_o \leq 106.86$ )

$$\frac{V_j}{V_{o,j}} = \frac{9.26}{x/r_o - 20.35} \quad j = 7$$

$$\frac{W_j}{r_o} = 0.78 \left( 53.7 + \frac{x}{r_o} \right) \quad j = 7$$

$$\frac{B_j}{r_o} = 0.592 \left( 54.44 + \frac{x}{r_o} \right) \quad j = 7$$

Fully Merged Column Jets ( $106.86 \leq x/r_o \leq x_{o,j}/r_o$ )

$$\frac{V_j}{V_{o,j}} = \frac{17.3}{(54.47 + x/r_o)^{1/2} (53.7 + x/r_o)^{1/2}} \quad j = 7$$

$$\frac{W_j}{r_o} = 0.78 \left( 53.7 + \frac{x}{r_o} \right) \quad j = 7$$

$$\frac{B_j}{r_o} = 0.592 \left( 54.44 + \frac{x}{r_o} \right) \quad j = 7$$

Transient Decay of End Cap Jet  $x_{o,j}/r_o \leq x/r_o \leq x_{t,j}/r_o$

$$\frac{v_j}{v_{o,j}} = \frac{v_{Q_o,j}}{v_{o,j}} \left[ 1 - \frac{2}{P_j} \frac{v_{o,j}}{v_{Q_o,j}} \left( \frac{x}{r_o} - \frac{x_{o,j}}{r_o} \right) \right]^{1/2} \quad j = 7$$

$$\frac{w_j}{r_o} = 0.78 \left( 53.7 + \frac{x}{r_o} \right) \quad j = 7$$

$$\frac{B_j}{r_o} = 0.592 \left( 54.44 + \frac{x}{r_o} \right) \quad j = 7$$

and

$$\frac{v_{Q_o,j}}{v_{o,j}} = \frac{2.94}{(P_j + 266.15)^{1/2}}$$

$$\frac{x_{o,j}}{r_o} = 5.882 (P_j + 266.15)^{1/2} - 54.09 \quad j = 7$$

$$\frac{x_{t,j}}{r_o} = \frac{x_{o,j}}{r_o} + \frac{1}{2} P_j \frac{v_{Q_o,j}}{v_{o,j}} \quad j = 7$$

and

$$P_j = \frac{v_{o,j} t_{o,j}}{r_o} \quad j = 7$$

A summary of the results is shown in Table A-3.

A4. DETERMINATION OF  $V_{o,j}$  AND  $t_{o,j}$ 

Before utilizing the modified T-quencher water jet model to evaluate the loads on submerged structures, the values of  $V_{o,j}$  and  $t_{o,j}$  for the water jet from each section of the quencher arm have to be determined.  $V_{o,j}$  is the orifice water velocity at Section  $j$  and  $t_{o,j}$  is the time at which the water flowing through the orifices in Section  $j$  stops.

The arm hole velocity and acceleration at the time when the air-water interface reaches the first column of holes on the quencher arm, are determined from the S/RV line clearing model output as follows:

$$\text{arm hole velocity, } V_{Ho} = FS \frac{\dot{m}}{\rho A_H} \quad (A1)$$

$$\text{arm hole acceleration, } \left( \frac{dV_H}{dt} \right)_o = FS \frac{\ddot{m}}{\rho A_H} \quad (A2)$$

where

FS = Flow split fraction between the two arms

$\dot{m}$  = Water mass flowrate, lbm/sec

$\ddot{m}$  = Water mass acceleration, lbm/sec<sup>2</sup>

$\rho$  = water density, lbm/ft<sup>3</sup>

$A_H$  = Flow area of all holes in one arm, ft<sup>2</sup>

The arm hole velocity  $V_H$  and the location of the air-water interface  $S$  (measured from the first column of holes) at any time are determined from the following equations:

$$V_H = V_{Ho} + \left( \frac{dV_H}{dt} \right)_o t \quad (A3)$$

$$C = \text{Exp} \left\{ \frac{2abt}{A_p} \left[ V_{Ho} + \frac{t}{2} \left( \frac{dV_H}{dt} \right)_o \right] \right\} \quad (A4)$$

$$S = \frac{a}{b} \frac{C - 1}{C + 1} \quad (A5)$$

where

$$a = \sqrt{A_H}$$

$b$  = Hole distribution coefficient

= 0.00952 for quencher with end cap holes

= 0.010024 for quencher without end cap holes

$A_p$  = Flow area of quencher arm,  $\text{ft}^2$

Solving  $t$  and  $C$  in terms of  $S$ , yields

$$C = \frac{\sqrt{A_H} + bS}{\sqrt{A_H} - bS} \quad (A6)$$

$$t = \frac{L}{V_{HO}} \frac{1}{\beta F_{vel}} \left\{ \sqrt{\beta^2 + 2\beta F_{vel} \ln C} - \beta \right\} \quad (A7)$$

where

$$\beta = \frac{2 \sqrt{A_H} L b}{A_P}$$

$$F_{vel} = \frac{L}{V_{Ho}^2} \left( \frac{dV_H}{dt} \right)_o$$

$L$  = Arm length from first column of holes to the end cap, ft.

Hence the arm hole velocity  $V_H$  can also be expressed as an explicit function of  $S$  by substituting Equation (A7) into Equation (A3).

The modified T-quencher water jet model divides the quencher arm into six sections as shown in Figure A1 and the orifice water velocity in Section  $j$  is taken to be the arm hole velocity at the time when the air-water interface reaches the last column of holes in Section  $j$  (i.e., when  $S = S_j$ , see Figure A1). If  $t_F$  (an output from the S/RV line clearing model) is the time that the air-water interface travels from its initial position to the first column of holes in the arm, then

$$t_{o,j} = t_F + t(S_j) \quad (A8)$$

is the time at which water flowing through the orifices in Section  $j$  stops. For a given set of initial conditions (i.e.,

$$V_{Ho}, \left( \frac{dV_H}{dt} \right)_o \text{ and } t_F,$$

the values of  $V_{o,j}$  and  $t_{o,j}$  for each section on the quencher arm can then be obtained through Equations (A3), (A6), (A7), and (A8).



TECHNICAL INFORMATION EXCHANGE

TITLE PAGE

AUTHOR	SUBJECT	TIE NUMBER
F. T. Dodge	730	79NED053
		DATE
		May 1979
TITLE		GE CLASS
Mark I - Analytical Models for T-Quencher Water Jet Loads on Submerged Structures		I
		GOVERNMENT CLASS
REPRODUCIBLE COPY FILED AT TECHNICAL SUPPORT SERVICES, R&UO, SAN JOSE, CALIFORNIA 95125 (Mail Code 211)		NUMBER OF PAGES
		73
SUMMARY		
<p>This document presents an analytical method to compute bounding loads on underwater structures due to water jets from a T-Quencher type S/RV discharge device. The general approach uses analytical and experimental results for steady-state jets that are available in open literature. A simple steady-state drag equation is used to predict the submerged-structure loads from the calculated velocities.</p>		
NEDO-25090		

By cutting out this rectangle and folding in half, the above information can be fitted into a standard card file.

DOCUMENT NUMBER NEDO-25090

INFORMATION PREPARED FOR Nuclear Energy Projects Division

SECTION Containment Improvement Programs

BUILDING AND ROOM NUMBER PYD 409 MAIL CODE 905

GENERAL  ELECTRIC

497 157